Proceedings of the 32nd European Safety and Reliability Conference (ESREL 2022)
Edited by Maria Chiara Leva, Edoardo Patelli, Luca Podofillini, and Simon Wilson
 Published by Research Publishing, Singapore.
doi: 10.3850/978-981-18-5183-4_R28-02-165-cd

Probabilistic approach for concrete structures exposed to combined carbonation-chloride-induced corrosion

P. Claude[a,b,c], F. Duprat[a], T. de Larrard[a], J. Mai-Nhu[b], P. Rougeau[b], L. Marracci[c], P. Guédon[c]

[a]*Université de Toulouse, LMDC INSA-UPS, duprat@insa-toulouse.fr, delarrar@insa-toulouse.fr*
[b]*CERIB Epernon, J.MAI-NHU@cerib.com, P.ROUGEAU@cerib.com*
[c]*Arcadis ESG, Paris, paulo.claude@arcadis.com, louis.marracci@arcadis.com, pascal.guedon@arcadis.com*

Corrosion of the steel reinforcements in concrete structures is a major cause of their deterioration. In most cases, corrosion is induced by carbonation or chlorination and only the supposedly prominent initiating phenomenon is considered. However, a combination of the two can be more uncertain because, in this case, both the chloride binding capacity and the pore microstructure of the cement paste are affected. The case of a concrete bridge subjected to carbonation and deicing salts is considered in this study. Specific Finite Element Modelling (FEM) was developed in order to estimate the time to reinforcement depassivation and the aim of the study is to estimate the probability of effective initiation of corrosion when the chloride content at the rebar surface exceeds a threshold value. The time, *t*, corresponding to this event, with a predefined probability, can be a significant milestone in the maintenance policy. Concrete properties, external environment (carbon dioxide pressure, chloride content, relative humidity) and concrete cover depth are considered as random variables in the study. In order to overcome the numerical weight of the FEM in the probabilistic computations, a surrogate model based on polynomial chaos expansion is employed. A Sobol sensitivity analysis is performed on the parameters to observe their influence on the result. Several locations are assumed for the structure, implying various environments and durations of the frost period. The results show that combined exposure to chlorides and carbon dioxide increases the depassivation rate and that the concrete cover thickness has the highest impact on the probability of depassivation.

Keywords: Carbonation, chlorination, corrosion, concrete structures, probabilistic approach, polynomial expansion, sensitivity analysis.

1. Introduction

Reinforced concrete is the most widely used construction material but its great versatility can make it complex to study and to model. The concrete protects the reinforcing bar from external aggressions and ensures an alkaline environment around the steel surface, causing its passivation [1]. Thus, the nature and design of the concrete cover influence the impact of major phenomena, such as carbonation induced corrosion or chlorination induced corrosion, on the reinforced concrete durability[2].

We recall that the total costs of corrosion, direct and indirect, represent between 2.5 and 4.5% of the world's GNP, corresponding to two thousand billion US dollars per year [3]. This point underlines the necessity to control and slow down this degradation process in order to reduce the costs associated with maintenance and repair. Moreover, corrosion is directly linked to safety issues since it may lead to failure of the structure.

The two main phenomena inducing corrosion in reinforced concrete are linked to the diffusion of aggressive species, chloride and carbon dioxide. Carbonation is a physicochemical process affecting the cementitious matrix of the concrete, which takes place in the presence of water (required for the dissolution of carbon dioxide) [4].

Portlandite ($Ca(OH)_2$) is one of the principal hydrates contained in concrete. It is mainly responsible for the basic pH value, generally between 12 and 13 in the cementitious matrix interstitial solution [5]. Passive films naturally

form on steel at pH values higher than 10.4, as when the steel is embedded in concrete [6]. While consuming the hydrates of the cementitious matrix, carbonation lowers the alkalinity of the interstitial solution. It may ultimately cause the destruction of the passive film and thus the initiation of corrosion [7].

Chloride penetration can also cause the passive film to break [8]. Chlorides are present in ionic form in the environment and penetrate the concrete by either diffusion or convection. In concrete material, chloride interacts with certain hydrates of the matrix and can be fixed by them. This property of the cementitious matrix, called its binding capacity, can slow the ingress of chloride into the material [9].

Once a certain concentration of free chloride ions is reached in the interstitial solution at rebar level, the passive layer dissolves, leaving the steel unprotected against corrosion. The critical concentration of chloride required to cause the initiation of corrosion at the rebar interface is a subject of debate. Values found in the literature vary from 0.03 % to 8.34 wt.% of the cement mass [10].

Through their impacts on the concrete microstructure and chemistry, the two phenomena described above can alter one another. First, carbonation reaction leads to a decrease of the concrete average porosity and, thus, to a decrease of the ability to transport chloride ions [11]. Second, carbonation may affect the hydrates of the cementitious paste, hindering their ability to bind chlorides once carbonated [12].

As stated earlier, the random variability of the concrete material and the environment to which the structure is exposed makes it necessary to consider uncertainties. When a deterministic approach is employed to evaluate the durability of a structure, simplifying assumptions are made to consider only the average values of the input parameters for a given model. Therefore, evaluation of the weak areas of a structure or of a singularity is impossible. For this reason, the use of a probabilistic or semi-probabilistic approach is often more advisable when the aim is to study the response of a concrete structure to its surrounding environment. Such approaches allow the variability to be taken into account by using probability distributions for the different parameters.

In a maintenance strategy, estimating the probability of corrosion initiation at the end of the designed service life, or the time when this probability exceeds a certain threshold is crucial.

2. Assessment Model

SDReaM-crete is a durability model developed jointly by the CERIB and the LMDC [7, 15]. It can predict carbonation, chloride penetration, and the corrosion induced by these two phenomena. The species considered are:

- hydrates of the cementitious matrix: portlandite (CH), calcium silicates (CSH), calcium monosulfates (Afm), ettringite (Aft);
- chloride ions: free chloride (Cl^-), physically bound chloride (YCSH) and Friedel's salt (FS);
- carbon dioxide (through the partial pressure of CO_2);
- oxygen (through the partial pressure of O_2);
- water (through the relative humidity);
- corrosion products (green rust and dense product layer).

Transfer equations of the different species are based on Fick's second law.

Partial differential equations are solved within the finite element software Comsol. From a more general point of view, SDReaM-crete involves:

- 45 constants (calibration, thermodynamic, physicochemical, etc.);
- 48 variables (microstructural parameters, durability coefficients, etc.);
- 47 equations (Arrhenius law, Van Genuchten equation, etc.).

However, the computational time (up to a few hours) is a severe constraint for the use of SDReaM-crete in the context of a probabilistic approach. In order to overcome this drawback, the present work has recourse to a surrogate model, mimicking the original one but based on a polynomial chaos expansion.

3. Case Conditions

The goal was to assess the impact of combined carbonation-chloride-induced corrosion on a reinforced concrete bridge subjected to deicing salt. The modelling conditions chosen to represent

the use of deicing salt on the structure were the following.

- First, annual variations for the relative humidity and the temperature were represented with a sinusoidal function (exposed in Eq. (4) for RH). This function was chosen arbitrarily to ease the modelling while considering a maximum and a minimum value. The parameters used to control the function were the average value of each function (μ_{RH} and μ_T) and the maximum variation (Δ_{RH} and Δ_T)

$$\boldsymbol{RH(t) = \mu_{RH} + \Delta_{RH}.\sin(2\pi t)} \quad (4)$$

- A single period of salting per year controlled by the maximum concentration value (C_{max}). The period of salting ($t_{salting} = t_2\text{-}t_1$) was represented with a square wave function (see Eq. (5)).

$$\boldsymbol{C_{env} = \begin{cases} 0 \; if \; t < t_1 \\ C_{max} \; if \; t_1 < t < t_2 \\ 0 \; if \; t > t_2 \end{cases}} \quad (5)$$

- Partial pressure of CO_2 was considered constant with time, and stated as a single average value μ_{CO_2}.

In Eqs. (4) and (5), t is the time in years. Boundary conditions were applied on one face of the structure while transfers were considered unidirectional.

4. Surrogate Models

A surrogate model (meta-model) created as part of the study gave the free chloride concentration at a certain depth as its output. To improve the accuracy and robustness of the surrogate model, an "average meta-model" was built from various Polynomial chaos expansions (PCE). The methodology is detailed in Section 4.2.

4.1. Input selection

The first step was the selection of the appropriate parameters. The variability of these parameters will therefore be considered in the probabilistic approach. It also implies the hypothesis that the remaining model parameters can be considered constant because their variability does not significantly affect the output. The parameters selected are meaningful to the study and their possible impact on the results is legitimized by the literature [7, 15]. Each data range was also established according to references and to enable consideration of the structure parts studied afterwards (see Table 1). The material used was CEM I-based concrete in each case. The structure is located in France.

The variation intervals of material parameters assume that the material employed for pre-stressed concrete bridge girders is a usual concrete. The variation of the environmental parameters is large enough for this aspect not to limit the use of the meta-model for a certain geographic zone.

In order to build the meta-model, a large number of computations had to be run with the original model. Latin Hyper-square Sampling (LHS) was used to improve the distribution of the dataset and maximise the overall training process [15].

Table 1. Input data range for building the meta-model

Var	Unit	Min	Max	Ref
ϕ	-	0.08	0.21	-
CH	mol/m^3	250	2000	[13]
CSH	mol/m^3	500	2200	[13]
Afm	mol/m^3	50	600	[13]
P_{CO2}	Pa	0	70	-
Kl1	m^2	10^{-19}	5.10^{-21}	-
RH	-	0.5	0.8	-
ΔRH	-	0.05	0.2	-
DCl	m^2/s	10^{-13}	10^{-11}	-
$t_{salting}$	Day	1	30	[14]
w/b	-	0.35	0.65	-
t_{tot}	Year	5	100	-
$[Cl]_{max}$	mol/m^3	40	2000	[14]
$[Cl]_{crit}$	mol/m^3	40	440	[8]

4.2. Polynomial chaos expansion (PCE)

PCE was selected as the type of meta-model and the python module OpenTURNS [16] was employed to compute the unknown coefficients of the PCE. The global functioning of this algorithm is described in this section.

First, the database of results is split into two datasets: the first (80%) serves to estimate (fit) the unknown coefficients of the meta-model. The second (20%) is dedicated to validating the meta-model by comparing the results obtained with the surrogate and the original models. These datasets are set randomly.

The goal of PCE is to model the response of a random output variable (Y) as a function of input

parameters ($X = \{x_1 \dots x_m\}$) through the general expression Eq. (6).

$$\boldsymbol{Y} = \sum_{\boldsymbol{\alpha} \in \boldsymbol{N}^{\boldsymbol{m}}}^{\infty} \boldsymbol{a}_{\boldsymbol{\alpha}} \boldsymbol{\psi}_{\boldsymbol{\alpha}}(\boldsymbol{X}) \quad (6)$$

$\boldsymbol{\psi}_{\boldsymbol{\alpha}}$ are the multivariate polynomials constituting the probabilistic space associated with the input parameters and $\boldsymbol{a}_{\boldsymbol{\alpha}}$ are the coefficients belonging to the real number [17].

Here, Legendre polynomials were used. This specific polynomial family is associated with uniform distributions of input data, which was the case for this work [18]. The coefficients $\boldsymbol{a}_{\boldsymbol{\alpha}}$ were determined through regression analysis: a truncation according to the expression $|\alpha| \leq p$ for the index α. To measure the performance of the model obtained with truncation, the second dataset was used. This method of cross validation, called "leave-one-out", allowed us to determine the coefficient Q^2 qualifying the generalization capability of the surrogate model. The value of Q^2 was between 0 and 1. The higher the value is, the better is the model performance [19].

The maximal PCE degree and its influence on the determination coefficient was studied to select the optimal configuration (see Fig. 1). The value taken for the maximal degree of each surrogate model was 12, which gave a determination coefficient sufficient for the application.

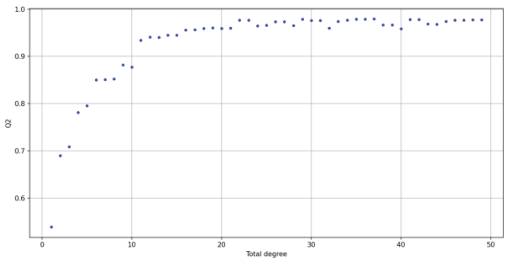

Fig. 1. Representation of the determination coefficients obtained for maximal polynomial order ranging from 1 to 50.

It can be highlighted here that there seems to be a threshold degree value for which the Q2 value ceases to increase. This certainly means that the new polynomial equations added to the PCE do not present any interest to improve the accuracy. Thus, the associated polynomial coefficients are equal to or close to zero.

The results obtained for the validation of the meta-model in the case studied here are plotted in Fig. 2.

As mentioned previously, an "average surrogate model" was formed from several meta-models. For this purpose, each meta-model was built from a new partition of the numerical design between the learning basis (size 7016) and the validation basis (size 1752). The polynomial coefficients obtained for each meta-model were then averaged in the final surrogate model (see Fig. 3). Meanwhile, the first and total Sobol indices were computed, together with the determination coefficient.

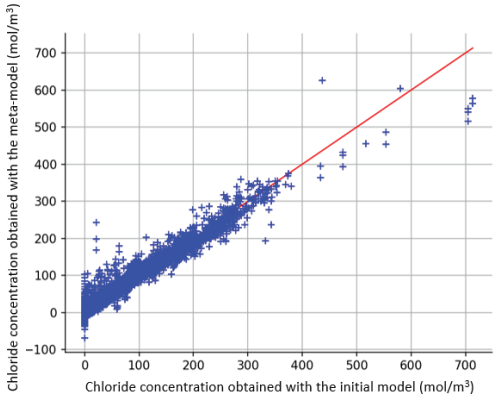

Fig. 2. Representation of one of the meta-model validations (Q^2=0.932).

4.3. Sobol sensitivity analysis

The Sobol sensitivity analysis emphasizes [20]:

- The influence of an individual parameter alone on the result with the computation of the first order index,
- The influence of a parameter and its interactions with the remaining input through the calculation of the total order index.

The first and total order indices were computed in this work.

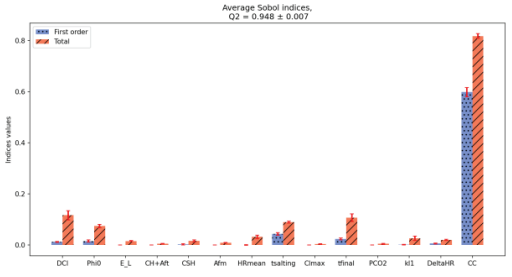

Fig. 3. Average values of the first and total order indices for the surrogate model computed.

5. Reliability Assessment

A first order reliability method (FORM) is used to compute the probability of failure [21]:

$$\boldsymbol{P_f = P(g(X,d) \leq 0) = \int_{D_f} f_X(x)dx} \quad (7)$$

where X is the input random vector, $f_X(x)$ the joint density probability function, $g(X, d)$ the limit state function of the model, and d a deterministic vector. The failure domain D_f is defined as:

$$D_f = \{X \in R^n / g(X, d) \leq 0\}.$$

Finally, the failure probability $\boldsymbol{P_{f,FORM}}$ can be obtained because the standard distribution f_U exhibits rotational invariance:

$$\boldsymbol{P_{f,FORM} = \begin{cases} \Phi(-\beta_{HL}) & \textit{if the origin of u\_space lies} \\ & \textit{in the safety domain } D_S = \overline{D_f} \\ \Phi(+\beta_{HL}) & \textit{otherwise} \end{cases}}$$

where $\boldsymbol{\beta_{HL}}$ is the Hasofer-Lind reliability index, defined as the minimum distance from the origin of the standard space to the failure surface G(U,d)=0, and $\boldsymbol{\Phi}$ is the standardized normal cumulative distribution.

In the present work, the failure criterion was expressed as

$$\boldsymbol{g = C_{crit} - [Cl^-]_{CC} \leq 0} \quad (8)$$

The Pearson correlation matrix of material parameters was accounted for and estimated from the PERFDUB database results [22]. Only the CEM I, filler and slag-based concretes were considered. The results are reported in Fig. 4. The other coefficients were considered equal to 0.

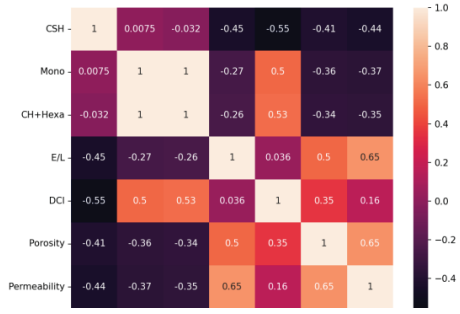

Fig. 4. Graphical representation of the correlation matrix obtained on the PERFDUB database.

6. Real Case Application

6.1. Durability design options

The data studied here were derived from different inspection tests carried out on a pre-stressed concrete bridge girder in the south of France. One beam (noted B1) and two struts (S1 and S2) of the same structure were considered. Durability design parameters, and concrete cover depth (*CC*), are reported in Table 2. Concrete cover measurements were performed with a cover meter at different locations along the structural components. From the measurements, a Beta distribution could be satisfactorily fitted and was adopted (see Fig. 5).

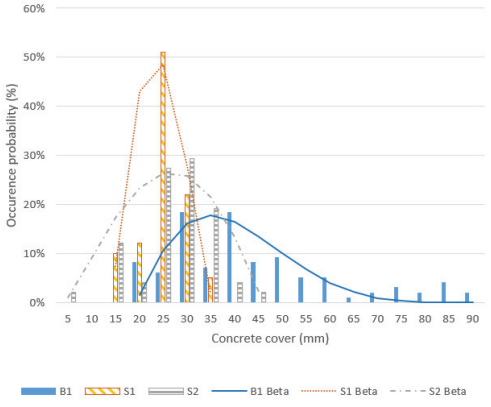

Fig. 5. Histograms and fitted Beta distributions for the concrete cover.

The parameters of the three distributions are reported in Table 2. The Beta distribution also has the advantage of being bounded on both sides, avoiding the occurrence of negative or excessive and unrealistic values for the concrete cover. In Table 2, a corresponds to the minimal value, b to the maximum value, and α and β to the distribution parameters [23].

Table 2. Durability parameters of the case study

Part	Cover (CC) (- - mm mm) (α-β-a-b)	w/b (-)	D_{Cl} (10^{-12} m^2/s)	φ (-)	K_{liq} (10^{-20} m^2)
B1	2.3 – 5.6 – 20 – 90	0.49	9.9	0.14	1.95
S1	2.2 – 2.7 – 15 – 35	0.6	15.0	0.17	4.88
S2	2.3 – 2.1 – 5 – 45	0.49	9.9	0.13	1.54

The distributions of the other parameters were defined either on the basis of experimental results (for w/b, porosity) or using models and data from the literature (for DCl, Kl, and concentrations of hydrates) [7]. The distributions are reported in Table 3. C_{crit} is considered constant and equal to 200 mol/m^3 to ease the comparison of the probability obtained. The choice of this value was based on the work of Schmitt [7].

Table 3. Durability design parameters for elements of concrete structure.

Parameter (distribution)	Statistical properties	Beam	Strut
DCl (Lognormal)	Mean (m^2/s)	Design	
	Deviation (m^2/s)	5.10^{-13}	
	Shift parameter (m^2/s)	10^{-13}	
Phi (Beta)	α	2.26	
	β	3.39	
	min (%)	μ_{design}-2	
	max (%)	μ_{design}+2	
K_{liq} (Normal)	Mean (m^2)	Design	
	Deviation (m^2)	10^{-20}	
w/b (Normal)	Mean (%)	Design	
	Deviation (%)	2	
CH + Aft (Beta)	α	2.57	
	β	6.43	
	min (mol/m^3)	μ_{design}-150	
	max (mol/m^3)	μ_{design}+150	
CSH (Beta)	α	10.89	
	β	12.93	
	min (mol/m^3)	μ_{design}-100	
	max (mol/m^3)	μ_{design}+100	
Afm (Beta)	α	2.5	
	β	5.83	
	min (mol/m^3)	μ_{design}-50	
	max (mol/m^3)	μ_{design}+50	
HR_{mean} (Normal)	Mean (%)	60	
	Deviation (%)	5	
$t_{salting}$ (Uniform)	Min	5	1
	Max	15	5
Cl_{max} (Normal)	Mean (mol/m^3)	500	250
	Deviation (mol/m^3)	100	100

Table 3. *(Continued)* Durability design parameters for elements of concrete structure.

Parameter (distribution)	Statistical properties	Beam	Strut
P_{CO2} (Normal)	Average (Pa)	50	50
	Deviation (Pa)	5	10
ΔHR (Normal)	Average (%)	15	10
	Deviation (%)	2.5	2.5

The strut surfaces are considered to be less exposed to environmental variations and aggressiveness than the beam surfaces, because of their "aerial" positions. For this reason, different values of $t_{salting}$, Cl_{max}, P_{CO2}, and ΔHR were chosen.

6.2. *Failure probability computation*

For the calculations of this section, a maximal duration of 100 years was chosen because it corresponds to the lifetime generally expected for this type of structure [24].

Failure probability (P_f) was computed for the three structural components. First, the evolution of P_f over time (from 50 to 100 years) is shown in Fig. 6.

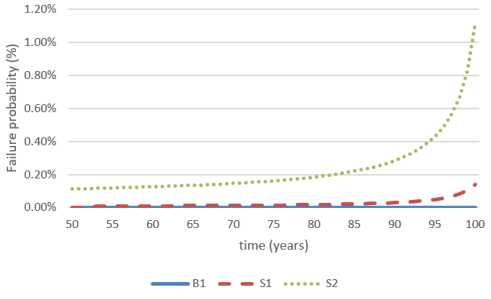

Fig. 6. Evolution of the failure probability vs. time for the different structural components.

It can be observed that the values obtained differ widely according to the structural component considered. Based on the Sobol indices obtained (see Fig. 3), the difference mainly originates in the concrete cover considered between components. Other materials and environmental parameters may also be influential, but to a lesser extent.

To compare the influence inherent in the other parameters, failure probabilities were also computed considering the same concrete cover distribution law for the three components. A Beta distribution law of parameters {α=2.5; β=2.5; min=μ_{CC} - 5; max= μ_{CC} + 5} was used, where μ_{CC}

is the average value of the concrete cover (mm) and corresponds to the value measured with the cover meter. μ_{CC} values ranging from 5 to 50 mm were considered. A time of 100 years was chosen here.

In addition, this second computation can be used to look at reliability results for a specific zone of the component (regarding the values measured with the cover meter presented in Section 6) instead of the overall element.

The results are reported in Fig. 7. Filled rectangles correspond to concrete cover values falling between the minimal and maximal measurements for the component while hashed rectangles refer to cover values smaller than the minimal value measured.

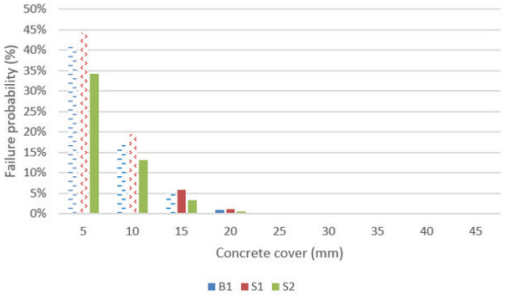

Fig. 7. Values of failure probability corresponding to a time of 100 years obtained for average concrete cover values ranging from 5 to 50 mm.

These results show that, when the same variation of the concrete cover is considered, the relative difference of failure probability obtained for the three components is reduced. This is in accordance with the results of the sensitivity analysis.

High values of failure probability are obtained on the part S2 for concrete cover (μ_{CC}) equal to 5 or 10 mm. This means that, on this structural component, if the zone considered for the concrete cover measurement is exposed to deicing salts at the same frequency as the one used for the computation, there is a high risk of depassivation of the rebar occurring.

The last aspect shown here is the impact of carbon dioxide. For the purposes of demonstration, different partial pressures of CO_2 were considered. Normal distributions were used with an average value of 50.5 and 70.5 Pa for the second and third cases. A constant value of 0 Pa was used in the first case (without carbonation). The failure probability was only calculated for S2.

The results obtained are represented as a function of time in Fig. 8.

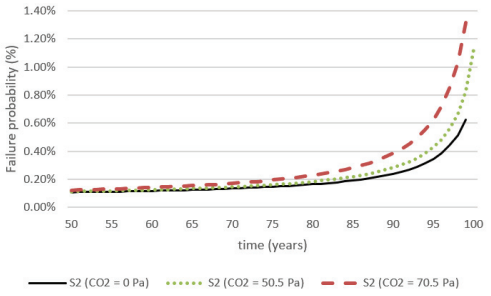

Fig. 8. Evolution of the failure probability through time for the structure part S2, considering different partial pressures of CO_2.

The results show a clear impact of the partial pressure as the failure probability increases with the partial pressure of CO_2. Here, the concrete cover considered is the one noted in Table 2 for structural part S2. Considering the capability of the initial model to represent reality fairly, these results prove that carbonation has an impact on chloride penetration, at least in the case of application of deicing salts to a structure. A link with the constantly increasing carbon dioxide pressure in the atmosphere due to human activity could also be made.

7. Conclusion

In this paper, a surrogate model has been established from a finite element model using a polynomial chaos expansion (PCE) method. The model is capable of computing chloride ingress in the case when deicing salt is spread on a reinforced concrete structure and of combining it with carbonation. It has been proven that the use of a PCE is efficient enough to obtain high values of determination coefficient (0.948 on average) using a maximal degree of 12 for the polynomial.

Once the surrogate model was established, it was possible to compute the first and total Sobol indices, which showed the impact of the different inputs on the result. The concrete cover value appears to be the most influential parameter.

A First Order Reliability Method was used considering different cases to highlight the facts that:

- Concrete cover variation indeed has the highest impact on the failure probability, which confirms the results of the sensitivity analysis

- For the conditions considered, concrete covers of 5 and 10 mm lead to elevated failure probability. These values are reassuring given the minimal value of 30 mm recommended in Eurocode 2 [24] for structures exposed to deicing salts.
- Partial pressure of CO_2 tends to increase the chloride penetration. This is in accordance with the fact that carbonation leads to the release of bound chloride in ionic form in the interstitial solution (free chloride) and reduces the binding capacity of the cementitious matrix.

Real measurements of the annual quantity and frequency of salting are difficult to obtain. Thus, the parameters used to fix the distribution law might need to be reviewed in order to obtain more accurate predictions on the structure.

References

1. Tuuti K, (1982) Corrosion of steel in concrete. Swedish Cement and Concrete Research Institute,Stockholm.
2. L'Hostis V et al. (2009) Characterization of long-term corrosion of rebars embedded in concretes sampled on French historical buildings aged from 50 to 80 years . Materials and Corrosion, vol.60, n°2, pp 93-98.
3. Moulinier F, (2010), How much does corrosion cost? TSM 7/8 - pp 26-38
4. Turcry P et al. (2014), Analysis of an accelerated carbonation test with severe preconditioning. Cement and Concrete Research, 57, pp 70-78.
5. Bullard J et al. (2011), Mechanisms of cement hydration. *Cement and Concrete Research*, 41(12), pp.1208-1223.
6. Lapuerta S (2005), Etude de la corrosion du fer à l'interface de différents milieux (eau, air) soumis à l'irradiation de protons. Thèse matériaux, Université Claude Bernard - Lyon I.
7. Schmitt L, (2019), Durabilité des ouvrages en béton soumis à la corrosion : optimisation par une approche probabiliste. PhD, LMDC Toulouse, France.
8. Schiessl
P, Lay S,(2005), « Corrosion in reinforced concret e structures », Corrosion in reinforced concrete stru ctures, edited by Hans Böhni, chapter 4 "Influence of concrete composition".
9. Hiro H et al.
(2005), « Chloride bonding of cement estimated b y binding isotherms of hydrates », Journal of Advanc ed Concrete Technology, 3, pp 77-84.
10. Angst U et al. (2009) Critical chloride content in reinforced concrete - A review. Cement and Concrete Research, 39, pp 1122-1138.
11. Hyvert N, (2009),
« Application de l'approche probabiliste à la durab ilité des produits préfabriqués en béton », PhD thesis,
Université de Toulouse in collaboration with CERIB.
12. Mai-Nhu J,
(2013), « Corrosion des armatures du béton : couplage carbonation/chlorures en présence*
de cycles hydriques », PhD thesis
Université de Toulouse III.
13. Kolani B, (2012), Comportement au jeune âge des structures en béton armé à base de liants composés aux laitiers . PhD thesis, Université de Toulouse.
14. Dossier d'organisation de la viabilité hivernale (DOVH) Direction interdépartementale des routes de l'Ouest
15. Stein M, (1987) Large Sample Properties of Simulations Using Latin Hypercube
Sampling, Technometrics, 29:2, pp 143-151
16. Baudin M et al. (2015). OpenTURNS: An Industrial Software for Uncertainty Quantification in Simulation. *Handbook of Uncertainty Quantification*, pp.1-38.
17. Blatman G, Sudret B, (2011). Adaptive sparse polynomial chaos expansion based on least angle regression. *Journal of Computational Physics*, 230(6), pp.2345-2367.
18. McClarren R, (2018). Stochastic Projection and Collocation. *Uncertainty Quantification and Predictive Computational Science*, pp.189-254.
19. Kersaudy P et al., (2013), Utilisation du chaos polynomial dans le cadre d'un problème d'homogénéisation, Journées scientifiques.
20. Damblin G, Ghione A, (2021). Adaptive use of replicated Latin Hypercube Designs for computing Sobol sensitivity indices. *Reliability Engineering & System Safety*, 212, pp.107-108.
21. Bai Y, Jin W, (2016). Basics of Structural Reliability. *Marine Structural Design*, pp.581-602.
22. Schober P et al. (2018). Correlation Coefficients. *Anesthesia & Analgesia*, 126(5), pp.1763-1768.
23. McDonald J, Xu Y(1995). A generalization of the beta distribution with applications. *Journal of Econometrics*, 66(1-2), pp.133-152.
24. Eurocodes 2 – norme NF EN 1992-2. Calcul des structures en béton Partie 1-1 : Règles générales
et règles pour les bâtiments, 2016 et Annexe Nationale à la NF EN 1992-1-1:2016 (2016).